International Journal of Science and Research (IJSR)
ISSN (Online): 2319-7064
Impact Factor (2012): 3.358

Three Dimensional Modeling of Water Erosion in the Fluid / Soil Interface

Kissi Benaissa[1], Parron Vera Miguel Angel[2], El Bakkali Larbi[3]

[1]National School of Arts and Trades of Casablanca, University Hassan II
Avenue Hassan II, B.P: 145, Mohammedia - Morocco,

[2]Mechanical and Civil Engineering Department, Polytechnic High School of Algeciras,
University of Cadiz, Ramon Pujol Avenue, Algeciras 11202

[3]Modeling and Simulation of Mechanical Systems Laboratory, Faculty of Sciences at Tetouan,
University Abdelmalek Essaadi, BP. 2121, M'hannech, 93002, Tetouan, Morocco,

Abstract: ***Soil erosion is a complex phenomenon which yields at its final stage insidious fluid leakages under the hydraulic infrastructures known as piping and which provokes their rupture. In this work, the water erosion is modeled in the fluid/soil interface during the hole erosion test (HET). The Hole Erosion Test is commonly used to quantify the rate of piping erosion. The aim of this work is to predict the erosion of soil in the fluid/soil interface by using the fluid package and three dimensional modeling. This modeling makes it possible describing the effect of the flow on erosion in the interface fluid/soil by using the*** $k-\varepsilon$ ***turbulence model equations, and predicts a non uniform erosion along the hole length unlike the usual one dimensional models. In particular, the flow velocity is found to increase noticeably the erosion rate. Effects on the wall-shear stress resulting from varying flow velocity and applied hydraulic gradient are analyzed. Various parametric studies were performed and had shown that the three-dimensional modeling introduced in the present study showed that the erosion rate is not uniform along the pipe wall as observed experimentally after performing the standard hole erosion test.***

Keywords: Piping, Soil erosion, Turbulence, $k-\varepsilon$ model, Near-wall boundary, Hole Erosion Test

1. Introduction

Soil erosion is a complex phenomenon which yields at its final stage insidious fluid leakages under the hydraulic infrastructures known as piping and which provokes their rupture. Many dam ruptures events have occurred throughout the world, some of them were reported by Foster and al. [1]. Then main cause was piping phenomenon that occurred in the foundation soil or in the dam structure. Serviceability of hydraulic infrastructures needs considering vulnerability of soil to internal erosion under the action of a seepage flow, [2,3]. Understanding the underlying mechanisms and quantifying the effects of pertinent variables that affect this phenomenon is of great importance in order to prevent such catastrophes. Erosion due to liquid flow discharge can be modeled by different approaches. These use some parameters that are identified from laboratory tests stating when erosion starts and what is the expected erosion rate. Among the most important tests that are used for this purpose, one finds the Hole Erosion Test (HET). A simplified one-dimensional model for interpreting the HET with a constant pressure drop was developed by Bonelli and Brivois [4,5]. This model yielded a characteristic erosion time which was found to be depending on the initial hydraulic gradient and the soil coefficient of erosion.

A two-dimensional modeling of fluid flow taking place in the hole inside the hole erosion test sample test was performed by means of enhanced CFD software package. The hole wall had been assumed to be rigid and to have ideal circular cylindrical geometry. Unlike the early models which are essentially one-dimensional, the two-dimensional modeling had shown that the wall-shear stress is not uniform along the hole wall [6]. Additional aspects due to two-dimensional features of the HET were observed during tests. For instance, the inlet side of the sample hole undergoes generally much more erosion than the outlet side. But, one-dimensional modeling of this test could not predict this eroded shape since it yields uniform erosion at the whole fluid/soil interface inside the soil sample hole.

The aim of this study is to describe the biphasic turbulent flow at the origin of erosion taking place inside the porous soil sample by considering the influence of variation of the flow velocity on rate erosion. A Computational Fluid Dynamics (CFD) approach is used to investigate the shear stress that develops at the water/soil interface and which represents the main mechanical action that causes surface erosion. The turbulence modeling of water flowing inside the hole of the HET sample was achieved by means of Fluent software package. This general purpose CFD code is especially appropriate for considering mixtures by modeling each fluid phase independently or as a homogenized medium, [7]. In this work, the modeling is performed by means of an improved version of the standard $k-\varepsilon$ model [reference of k epsilon model]. When the shear stress is calculated by means of Fluent, the classical linear erosion law is used to estimate erosion rate. This law gives erosion rate, considered to be the amount of mass departure due to erosion per unit time and by unit surface area, by $\dot{\varepsilon}_{er} = c_{er}(\tau - \tau_{cr})$ where c_{er} and τ_{cr} are constants depending on the considered soil material. For a cylindrical hole, the rate $\dot{\varepsilon}_{er}$ can be related to time variation of local radius by $\dot{\varepsilon}_{er} = \rho_d dR/dt$ where ρ_d is the dry density of soil and R is hole radius. The erosion law yields that $\dot{\varepsilon}_{er}$

is proportional to the amount of shear exceeding the critical shear τ_{cr} for which erosion begins.

The standard HET is such that, the fluid domain which is assumed to be axisymmetric extends over 117 mm in the axial z-direction and 3 mm in the radial r-direction, figure 1.

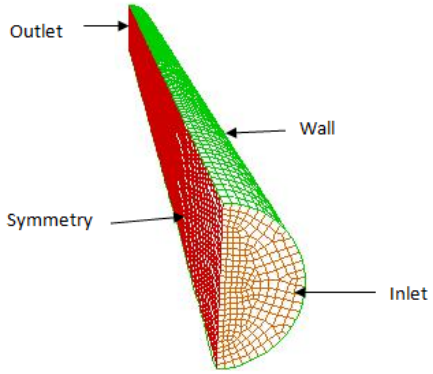

Figure 1: Geometry of the HET tube

2. The standard Hole Erosion Test

Several experiments were designed to reproduce in laboratory conditions surface erosion mechanisms taking place at the fluid/soil interface during piping. Recently, the Hole Erosion Test was introduced, [8]. This test proved to be simple, fast, and well adapted to perform surface erosion characterization during piping development for all investigated cases. The HET consists in introducing inside a standard mould a cylindrical sample of soil that is to be tested against surface erosion. The sample length is $L = 117\ mm$. A cylindrical hole of radius $R = 3\ mm$ is perforated along the longitudinal axis of the cylinder. A constant hydraulic head is applied between the tube extremities.

Theoretical modeling of the HET test has been performed under some assumptions [9-10]. A simplified modeling of the HET was introduced in [11]. These models, which are essentially one-dimensional, proved to be sufficient in explaining the erosion phenomenology related to piping problem. They yield a comprehensive description of the erosion initiation and kinetics for a given soil. These rudimentary models enable also to evaluate the influence of the hydraulic conditions on the kinetics and to quantify the gain in time left to rupture by operating for example partial drainage of the water reserve. In one-dimensional modeling and two-dimensional modeling, the surface erosion law is stated traditionally, [6,8], to be given by $\dot{\varepsilon}_{er} = c_{er}(\tau - \tau_s)$, where $\dot{\varepsilon}_{er}$ is the erosion rate which corresponds to the mass loss per unit time and per unit surface area, c_{er} is the surface erosion coefficient which measures the soil erodability, τ is the actual shear stress acting at the wall (assumed to be constant along the whole hole length) and τ_s is the shear erosion threshold limit.

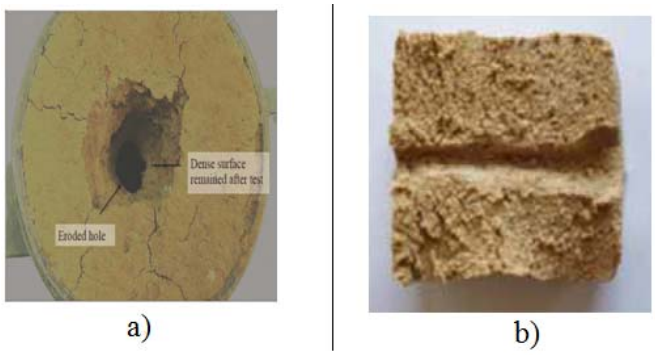

Figure 2: Sample tested with the HET

The erosion happens only if τ exceeds in absolute value τ_s. By using mass conservation of soil, one could easily arrive at $\dot{R} = \dot{\varepsilon}_{er} / \rho_d$ where ρ_d is the dry density of soil sample and R the actual radius of the tube, [11]. This last relation predicts uniform radius along the hole during erosion. Additional aspects associated to the three-dimensional nature of the HET are present in the problem. Figure 2) presents a meridian section of the tested sample after performing the test. It shows that the inlet side (right) of the hole has undergone much more erosion than the outlet side (left). As seen previously one-dimensional modeling of this test could not predict this eroded shape since it yields uniform erosion at the water/soil interface.

3. Three-dimensional modeling approach of the HET

The turbulence modeling is achieved by means of fluent software package. Fluent is a general purpose Computational Fluid Dynamics (CFD) code that has been applied to various problems in the fields of fluid mechanics and heat transfer. This code has been validated through numerous investigations. Fluent is especially appropriate for the complex physics involved in heat and mass transfer and considers mixtures by modeling each fluid species independently or as a homogenized medium, [12].

FLUENT is a 3 Dimensional, finite volume computational fluid dynamics code. The code can handle fully unstructured 3D tetrahedral volume meshes, along with 2 dimensional, and 3 dimensional structured meshes. It can handle both steady-state and transient analysis types, and is capable utilizing several different types of turbulence modeling. Using the finite volume method, FLUENT solves for the conservation of both mass and momentum in all fluid flow cases. Flow taking place inside the hole is turbulent. To perform realistic simulation of turbulence, the exact instantaneous Navier-Stokes governing equations are habitually time-averaged or ensemble-averaged. The obtained averaged equations contain further unknown variables, and turbulence models are introduced to determine them in terms of known quantities. Various turbulence models have been proposed in the literature; however there is no single turbulence model which could be universally applied for all classes of problems. The choice of a pertinent model for a given problem will depend on the actual physics of the flow, the degree of accuracy required and the computational cost tolerated. Reference [7] gives a detailed

discussion on how to perform at best the appropriate choice of a turbulence model. Among the various models, the standard $k-\varepsilon$ model which was proposed first by Launder and Spalding [13] has become the most popular when dealing with practical engineering flow calculations. This model relies on phenomenological considerations and integrates empiricism to perform closure of equations.

4. K-Epsilon Turbulence model

The standard k-epsilon model is a simple yet robust two-equation turbulence model that has been utilized widely in industry for practical flow analyses over the years.

The standard k – ε Model [13] is based on the Bousinesq concept (1977). The Reynolds stresses terms are:

$$-\rho\overline{u_i u_j} = 2\mu_i s_{ij} - \frac{2}{3}\rho k\delta_{ij} \quad (1)$$

With:

$$s_{ij} = \frac{1}{2}\left(\frac{\partial U_i}{\partial x_j} + \frac{\partial U_j}{\partial x_i}\right) \quad ;$$

$$\mu_t = \rho\nu_t = \rho C_\mu \frac{k^2}{\varepsilon}$$

With

$$C_\mu = 0.09$$

The turbulent kinetic energy is defined by:

$$k = \frac{1}{2}\overline{u_i u_i} = \frac{1}{2}\left(\overline{u_1^2 + u_2^2 + u_3^2}\right) \quad (2)$$

The turbulent energy dissipation rate ε is defined by:

$$\varepsilon = \nu\overline{\frac{\partial u_i \partial u_j}{\partial x_j \partial x_j}} \quad (3)$$

The $k-\varepsilon$ model constants have values derived analytically by the $k-\varepsilon$ theory [13] .They are given by:

Table 1: Values of the k – ε model constants

C_μ	$C_{\varepsilon 1}$	$C_{\varepsilon 2}$	σ_k	σ_ε
0.09	1.44	1.92	1	1.3

It is essential to know that the k-ε model is applicable to flows at high Reynolds number. These default values have been determined from experiments with air and water for fundamental turbulent shear flows including homogeneous shear flows and decaying isotropic grid turbulence. They have been found to work fairly well for a wide range of wall-bounded and free shear flows.

4.1 Standard k-ε Model

The simplest "complete models" of turbulence are two-equation models in which the solution of two separate transport equations allows the turbulent velocity and length scales to be independently determined. The standard k-ε model in FLUENT falls within this class of turbulence model and has become the workhorse of practical engineering flow calculations in the time since it was proposed by Launder and Spalding [13]. Robustness, economy, and reasonable accuracy for a wide range of turbulent flows explain its popularity in industrial flow and heat transfer simulations. It is a semi-empirical model, and the derivation of the model equations relies on phenomenological considerations and empiricism.

As the strengths and weaknesses of the standard k-ε model have become known, improvements have been made to the model to improve its performance. Two of these variants are available in FLUENT: the RNG k-ε model [14] and the realizable k-ε model [15].

The standard k- ε model [13] is a semi-empirical model based on model transport equations for the turbulence kinetic energy (k) and its dissipation rate (ε). The model transport equation for k is derived from the exact equation, while the model transport equation for ε was obtained using physical reasoning and bears little resemblance to its mathematically exact counterpart.

In the derivation of the k- ε model, the assumption is that the flow is fully turbulent, and the effects of molecular viscosity are negligible. The standard k- ε model is therefore valid only for fully turbulent flows.

4.2 Transport Equations for the Standard k-ε Model

The turbulence kinetic energy, k, and its rate of dissipation, ε, are obtained from the following transport equations:

$$\frac{\partial}{\partial t}(\rho k) + \frac{\partial}{\partial x_i}(\rho k u_i) = \frac{\partial}{\partial xj}\left[(\mu + \frac{\mu_t}{\sigma_k})\frac{\partial k}{\partial x_j}\right] + G_k + G_b - \rho\varepsilon - Y_M + S_k \quad (4)$$

and

$$\frac{\partial}{\partial t}(\varepsilon\rho) + \frac{\partial}{\partial x_i}(\rho\varepsilon u_i) = \frac{\partial}{\partial xj}\left[(\mu + \frac{\mu_t}{\sigma_\varepsilon})\frac{\partial \varepsilon}{\partial x_j}\right] + C_{1\varepsilon}\frac{\varepsilon}{k}(G_k + C_{3\varepsilon}G_b) - C_{2\varepsilon}\rho\frac{\varepsilon^2}{k} + S_\varepsilon \quad (5)$$

In these equations, G_k represents the generation of turbulence kinetic energy due to the mean velocity gradients. G_b is the generation of turbulence kinetic energy due to buoyancy. Y_M represents the contribution of the fluctuating dilatation in compressible turbulence to the overall dissipation rate. $C_{1\varepsilon}$, $C_{2\varepsilon}$, and $C_{3\varepsilon}$ are constants. σ_k and σ_ε are the turbulent Prandtl numbers for k and ε, respectively. Sk and S_ε are user-defined source terms.

Although the default values of the model constants are the standard ones most widely accepted, you can change them (if needed) in the Viscous Model panel.

5. Results and Discussions

The analysis presented in this section focuses on the simulation of the turbulent fluid flow taking place inside a cylindrical pipe having a rigid wall that replicates the geometry of the hole in the HET. The fluid domain which is assumed to be axisymmetric extends 170 mm in the axial z-direction and 30 mm in the radial r-direction. The origin of the reference frame is placed at the entrance section.

Figure 3 shows the obtained mesh that was transferred to Fluent.

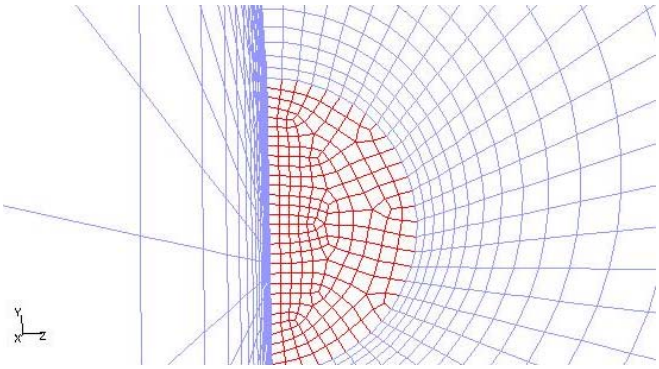

Figure 3: HET tube Disretized fluid domain with a zoom showing the grading cells in the radial direction

Modeling under fluent has been performed by using water density and dynamic viscosity at the temperature 20°C for which $\rho = 1000\ kg/m^3$ and $\eta = \rho\mu = 0.001\ Pa.s$. The four values of flow considered are given in table 2:

Table 2: Reynolds number and velocity of flow considered in this study

Reynolds	Velocity (m/s)	Debit. 10^{-5} (m^3/s)	T.I(%)
3000	0.5	1.413	5.8
7000	1.17	3.3	5.3
14000	2.34	6.61	4.9
20000	3.34	9.43	4.6

The solution method chosen under Fluent is Volume Of Fluid (VOF). The viscous Model selected is the standard $k-\varepsilon$ model and the near-wall treatment is conforming to the enhanced wall treatment with pressure gradient effects.

The boundary conditions that were used are:

- Inlet at the left extremity of the domain with gauge pressure value specified and turbulence specification method corresponding to turbulence intensity T.I(%) and hydraulic diameter equal to the radius R. turbulence intensity can be calculated as: $T.I = 0.16 \times \mathrm{Re}^{-1/8}$
- Outlet at the right extremity of the domain with gauge pressure fixed at 0, turbulence specification method was used with turbulence intensity T.I(%) and hydraulic diameter equal to the radius R.
- Symmetry type axis at the axis of symmetry which is the bottom side of the domain as presented in figure 1.
- Wall at the top side of the domain, figure 1, where the enhanced near-wall treatment with pressure gradient effects option is selected.

Default convergence statements were selected. They assure that continuity, velocities, turbulent kinetic energy and its dissipation rate are stationary within a relative tolerance limit fixed at 10-6.(Figure 4).The solution converges in approximately 290 iterations. The residuals plot is shown in Figure 4.

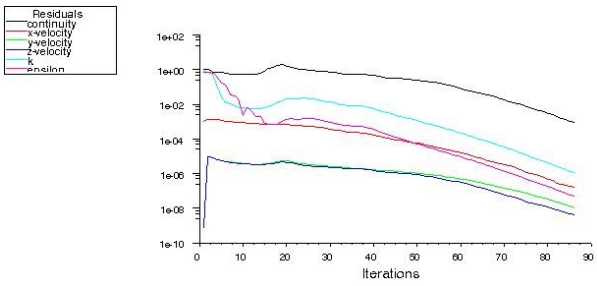

Figure 4: Scaled Residuals

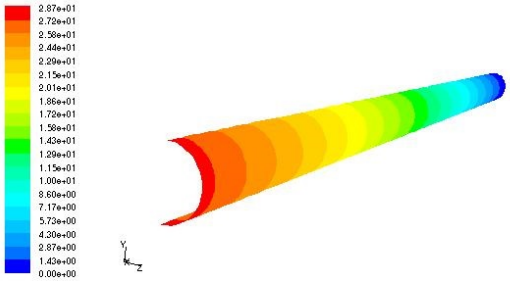

Figure 5: Contours of static pressure on wall for Re=3000

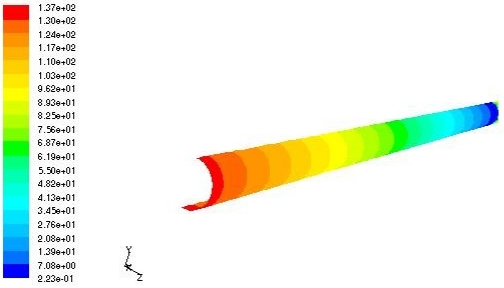

Figure 6: Contours of static pressure on wall for Re=7000

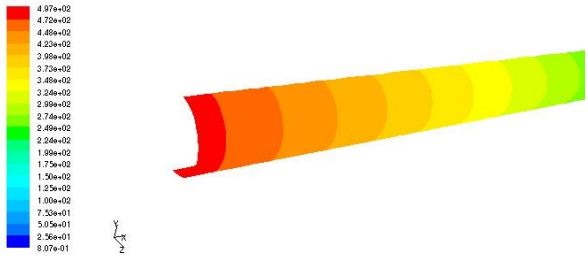

Figure 7: Contours of static pressure on wall for Re=14000

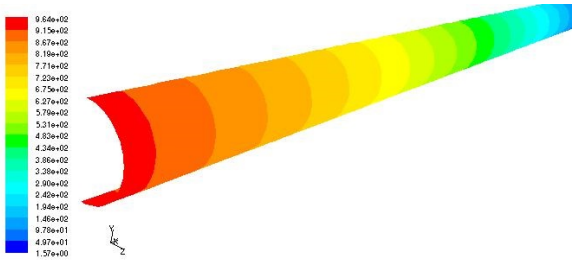

Figure 8: Contours of static pressure on wall for Re=20000

Figures 5,6,7,8 give the Contours of static pressure on wall as function of Reynolds number.
Figures 9,10,11,12 give the Contours of radial velocity on symmetry as function of Reynolds number.
Figures 13,14,15,16 give the Profiles of Wall Shear Stress on wall as function of Reynolds number.

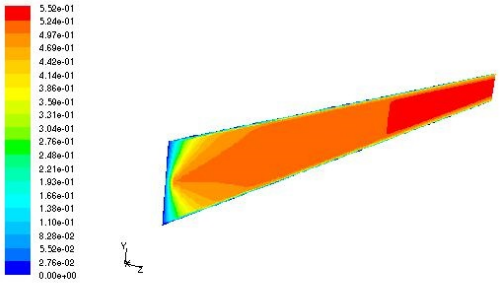

Figure 9: Contours of radial velocity on symmetry for Re=3000

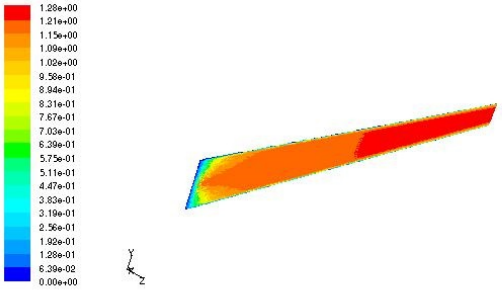

Figure 10: Contours of radial velocity on symmetry for Re=7000

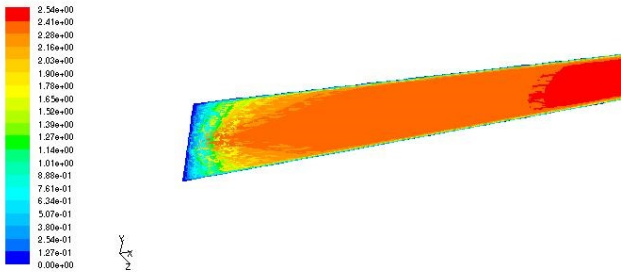

Figure 11: Contours of radial velocity on symmetry for Re=14000

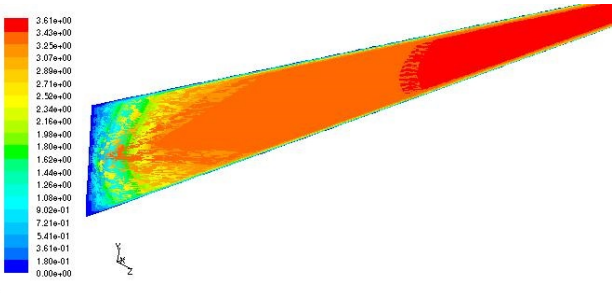

Figure 12: Contours of radial velocity on symmetry for R=14000

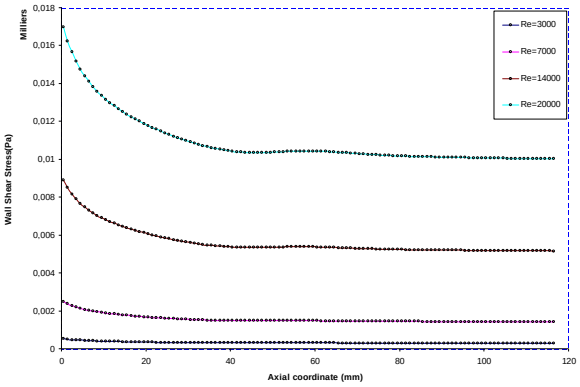

Figure 17: Wall-shear stress obtained as function of Reynolds number

Table 3 gives the erosion rate (in $10^{-4}\ kg/s$) which corresponds to the amount of mass departure per unit time due to erosion. This amount is obtained by integrating the erosion law over the whole length of the hole and by multiplying the result by the initial circumference of the hole. The classical linear erosion law $\dot{\varepsilon}_{er} = c_{er}(\tau - \tau_s)$ was used, with the erosion constants $c_{er} = 5.5\times10^{-4}\ s/m$ and $\tau_s = 0.2\ Pa$ as identified for a soil sample containing 50% kaolinit clay and 50% of sand that was tested in [19].

Table 3: Erosion rate in 10^{-4} kg / s as function of Reynolds number

Re	τ (Pa)	$\dot{\varepsilon}_{er}$
Re=3000	0.52	1.6
Re=7000	2.48	12.5
Re=14000	8.9	47.8
Re=20000	17	92.2

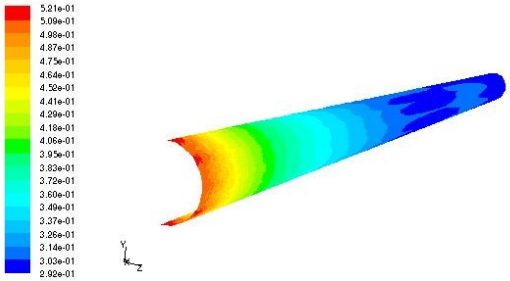

Figure 13: Profiles of Wall Shear Stress on wall for R=3000

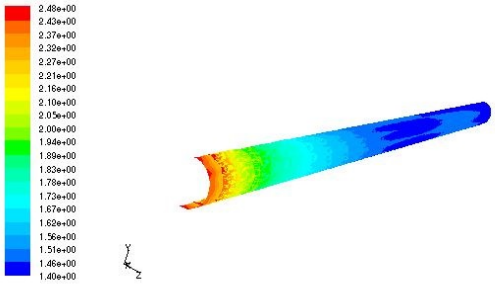

Figure 14: Profiles of Wall Shear Stress on wall for Re=7000

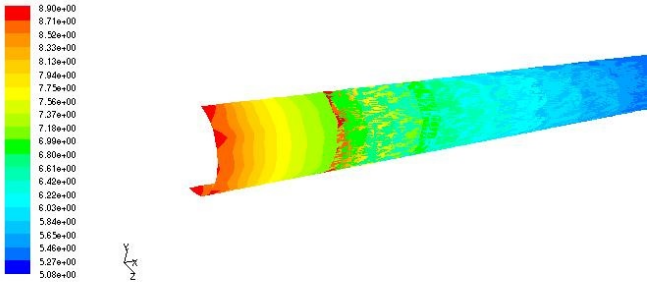

Figure 15: Profiles of Wall Shear Stress on wall for Re=14000

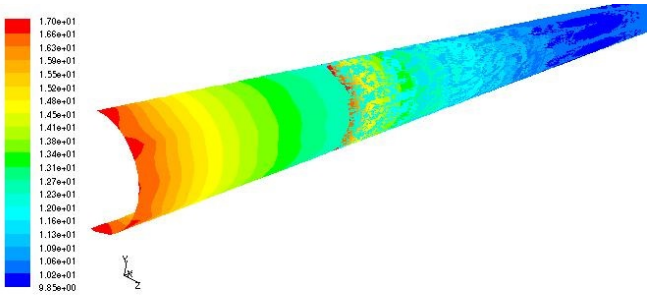

Figure 16: Profiles of Wall Shear Stress on wall for Re=20000

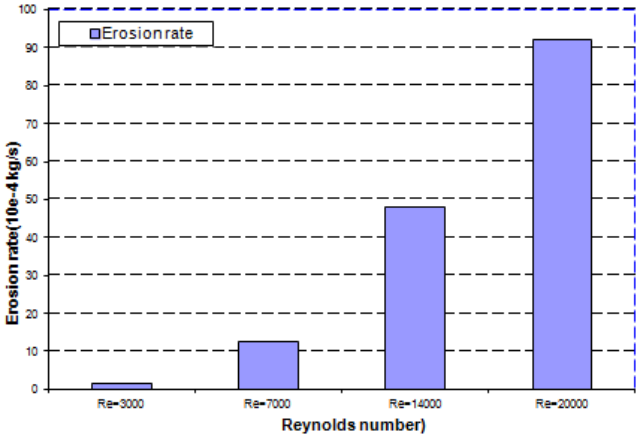

Figure 18: Erosion rate as function of inlet velocity (Reynolds number)

Figures 13, 14, 15, 16 and 17 show that the wall-shear is not uniform along the whole hole length. The wall-shear stress at the inlet extremity can exceed multiple times its permanent value in the plateau zone inside the hole. This is in contrast with the habitual hypothesis used to derive one-dimensional modeling of the HET. The obtained results, as shown in figure 18, indicate that erosion rate increase with Reynolds number and wit the axial coordinate.

In figures 5, 7, 8 and 9 shows that pressure is not linearly varying along the hole length. The obtained results state clearly the three-dimensional character of flow taking place inside the hole and show strong variations in comparison with two-dimensional and one-dimensional approaches. Predicting the erosion in its initial stage can be done under the assumptions that the wall is rigid and that the linear erosion law is valid. This was performed and results are summarized in table 3 where it could be observed that the Reynolds number has strong effect on the amount of erosion rate. The erosion rate increases as function the flow velocity with a maximum value at the inlet extremity. at the inlet extremity wall-shear stress is maximal and erosion is maximal.

6. Conclusions

A three-dimensional modeling of fluid flow taking place in the hole inside the hole erosion test sample test was performed by means of enhanced CFD software package. The hole wall had been assumed to be rigid and to have ideal circular cylindrical geometry. Unlike the early models which

are essentially one-dimensional, the three-dimensional modeling had shown that the wall-shear stress is not uniform along the hole wall (in the water/soil interface). It was possible then through using a linear erosion law to predict non uniform erosion along the hole length. Studying the effect of Reynolds number has shown that it has important effect on the wall-shear stress and thus would affect in its turn surface erosion that develops at the fluid soil sample interface. This enabled qualitatively understanding why the eroded profile of the hole wall as observed during experiment is not uniform.

The modeling performed in this work has limitations since the hole wall was modeled to be rigid and perfectly waterproof while in reality the soil sample is deformable and the interface is traversed by a Darcy like flow. It would be interesting in the future to examine how the deformation of the tube can affect the fluid flow by developing an enhanced model which takes into account coupling in a more complete manner between the flow and the soil sample.

References

[1] M.A. Foster, R. Fell, M. Spannangle. The statistics of embankment dam failures and accidents. Canadian geotechnical Journal 37 (2000) 100-1024.
[2] Fjar E., Holt R.M., Horsrud P., Raaen A.M., Risnes R., Petroleum related rock mechanics, revised edition Elsevier, Amsterdam, 2004.
[3] Lachouette D. Golay F., Bonelli S. One dimensional modelling of piping flow erosion. C. R. Mecanique 336 (2008) 731–736.
[4] D. Lachouette, F. Golay, S. Bonelli. One dimensional modelling of piping flow erosion. Comptes Rendus de Mécanique 336 (2008), 731-736.
[5] S. Bonelli, O. Brivois. The scaling law in the hole erosion test with a constant pressure. International Journal for Numerical and Analytical Methods in Geomechanics, 32(2008) 1573-1595.
[6] Kissi Benaissa, Parron Vera Miguel Angel, Rubio Cintas Maria Dlolores, Dubujet Philippe, Khamlichi Abdellatif, Bezzazi Mohammed, El Bakkali Larbi. Predicting initial erosion during the Hole Erosion Test by using turbulent flow CFD Simulation. Applied Mathematical Modelling. 36 (2012) 3359–3370
[7] Fieldview reference Manual, Software Release Version 10, Intelligent Light, 2004.
[8] C.F. Wan, R. Fell. Investigation of rate of erosion of soils in embankment dams, Journal of Geotechnical and Geoenvironmental Engineering, 30(2004) 373-380.
[9] S. Bonelli, O. Brivois, R. Borghi, N. Benahmed. On the modelling of piping erosion. C.R. Mécanique, 22 (2006) 225-244.
[10] S. Bonelli, O. Brivois. The scaling law in the hole erosion test with a constant pressure. International Journal for Numerical and Analytical Methods in Geomechanics, 32(2008) 1573-1595.
[11] A. Khamlichi, M. Bezzazi, L. El Bakkali, A. Jabbouri, B. Kissi, F. Yakhlef, M.A. Parron Vera, M.D. Rubio Cintas, O. Castillo Lopez. Modelado analítico simplificado del ensayo normal de erosión de tubo. Ingeniería Civil 155 (2009) 81-85.
[12] A. Escue, J. Cui. Comparison of turbulence models in simulating swirling pipe flows. Applied Mathematical Modelling. (2010) doi:10.1016/j.apm.2009.12.018.
[13] Launder, B.E., Spalding, D.B. Lectures in Mathematical Models of Turbulence. Academic Press, London, England, 1972.
[14] V. Yakhot and S. A. Orszag. Renormalization Group Analysis of Turbulence: I. Basic Theory. Journal of Scientific Computing, 1(1):1-51, 1986.
[15] T.-H. Shih, W. W. Liou, A. Shabbir, Z. Yang, and J. Zhu. A New k-ε Eddy-Viscosity Model for High Reynolds Number Turbulent Flows - Model Development and Validation. Computers Fluids, 24(3):227-238, 1995.
[16] D.Choudhury. Introduction to the Renormalization Group Method and Turbulence Modeling. Fluent Inc. Technical Memorandum TM-107, 1993.
[17] S.B. Pope. Turbulent flows. Cambridge University Press, 2000.
[18] Fluent 6.2 Users Guide. Fluent Inc., 2005.
[19] T.L. PHAM. Erosion et dispersion des sols argileux par un fluide. In French. Ph.D Thesis, Order number: D.U. ED: 430. Ecole Nationale des Ponts et Chaussées, Paris, France, 2008.

Author Profile

He is a Professor at National School of Arts and Trades of Casablanca, University Hassan II, Morocco. He is a civil engineer. His Phd degree was graduated from University of Cadiz, in Spain and University Abdelmalek Essaadi from Morocco in 2011.